International Journal of
INTELLIGENT SYSTEMS AND APPLICATIONS IN ENGINEERING
ISSN:2147-6799 www.ijisae.org Original Research Paper

Detection of Brain Tumor from MRI Images Using Deep Dense Neural Network

[1] B. Thimma Reddy, [2] Dr V. V. S. S. S. Balaram

Submitted: 25/04/2023 **Revised**: 26/06/2023 **Accepted**: 07/07/2023

Abstract: The classification of Brain tumors is fundamental for the finding of Brain Cancer (BC) in medical services frameworks. AI (artificial intelligence) methods in light of PC-supported analytic frameworks (Miscreants) are generally utilized for the exact location of brain tumors. In any case, because of the issues like the mistake of counterfeit demonstrative frameworks, clinical experts are not really integrating them into the conclusion cycle of Brain tumors (BT). As deep learning (DL) technology got revolutionized greatly in medical fields, the usage of such ideas brings more effectiveness in terms of performance and accuracy. With that said, this research work offers an efficient deep learning-based categorization of brain tumors, with the steps being as follows: a) Data collecting from well-known databases for the brain, lung, and liver, which together comprise 10,000 records, b) Preprocessing using CLAHE (for brightness enhancing), Thresholding (Grayscale), Filtering (ADF) and skull masking for removal of noise and anomalies from raw images, c) feature extraction using Principle Component Analysis (PCA), d) feature selection using VGG16 network and finally e) classification using Deep Dense Neural Network (Densenet 164). Experimental tests indicates that the proposed model outperforms better than other state-of-art models under different measures (accuracy: 0.97, sensitivity: 0.98, specificity: 0.98, detection rate: 0.94).

Keywords: *ADF, Classification, CLAHE, Deep learning, Deep dense neural network, Grayscale, PCA*

1.Introduction

The most fatal brain disorders that can arise from aberrant cell growth inside the skull are brain tumors. 70% of all cancer cases are primary brain tumors, which damage the brain. Secondary brain tumors start in a different organ, like the breast, kidney, or lung, and then spread to the brain. Nearly 29,000 primary brain tumor cases are diagnosed in the US alone each year, and 13,000 people passed away as a result, according to the NBTF report [1]. Similar numbers show that over 42,000 individuals with primary brain tumors pass away annually in the UK. The three main types of brain tumors are “gliomas, meningiomas, and pituitary tumors”. The uncontrolled proliferation of glial cells, which make up about 75% of the brain, causes glioma tumors. It has the highest mortality rate when compared to other primary cancers. This gland creates many essential hormones. Despite being benign, the pituitary tumor can lead to hormonal imbalances and irreversible eyesight impairment [2]. In order to shield patients from negative effects, it is crucial to make an early and correct diagnosis of BT [3]. Different medical imaging technologies used for diagnosing brain tumors depending on their goal. [4]. Magnetic Resonance Imaging (MRI), which examines without the use of hazardous ionizing radiation like X-rays, is the most widely used noninvasive imaging tool. It also produces sharp images of soft tissues and can capture modalities utilizing a range of parameters, including FLAIR, T1, and T2 [5]. Figure 1 displays a brain tumor block diagram based on deep learning.

Because tumors often vary in form, severity, size, and location, it can be difficult to determine the type of a certain tumor. Usually, after thoroughly examining the photographs, the medical personnel meticulously mark out the tumor spots. Tumor borders are generally hidden by the healthy tissues that surround them. This makes the manual visual inspection identification process time-consuming and liable to tumor misunderstanding. Additionally, the radiologist's experience is essential for manually detecting tumors [6]. It should be noted that different shades of gray seen in MRI scans cannot be seen by the naked eye. Radiologists who are too tired to read MRIs or noisy MRIs brought on by differences in imaging equipment are two more common causes of tumor misinterpretation. In order to decrease the likelihood of a biopsy, radiologists could use automated techniques to visually assess the depth of the tumor or to determine the type of tumor [7, 8]. Brain tumor detection techniques based on CAD have been proposed by numerous researchers. The drawback of conventional Machine learning algorithms is that they rely on a manual feature extraction method. Before classification, the features are retrieved from training images [9].

[1] *Research Scholar in Department of CSE, Anurag University, Telangana, Associate Professor in CSE, G.Pulla Reddy Engineering College, Andhra Pradesh*

[2] *Professor, Department of CSE, Anurag University, Telangana, vbalaram23@gmail.com*

** Corresponding Author Email: thimmareddybuchi@gmail.com*

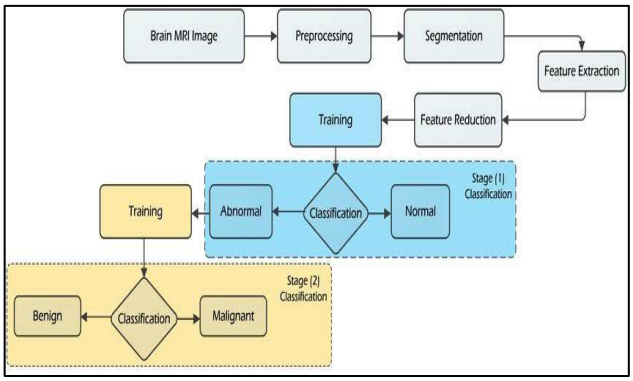

Fig 1. Systematic legacy diagram of brain tumor classification

ML and DL-based methods can be used to classify brain tumors. Prior to classification, ML-based systems perform labor-intensive, error-prone manual segmentation and feature extraction. To choose the appropriate feature for accurate cancer identification, extraction, and segmentation, algorithms frequently require the assistance of a specialist with in-depth knowledge. As a result, these systems' performance is unstable when dealing with bigger databases [10]. On the other hand, DL-based algorithms automate these procedures and have proven to be very beneficial in a variety of applications, including medical image analysis. From training data, it can automatically extract both low-level and high-level attributes. As a result, scientists and researchers are interested in these strategies [11].

1.1 Key Highlights

This research work focuses on bringing an effective deep learning model for a brain tumor, in which following are the objectives:

- Develop an accurate classifier for detecting multi-disease brain tumor.
- With the help of a custom dataset taken from a popular repository for effectively train and test the model
- The feature extraction and selection stage bring a boost to the overall classifier to improve the performance.
- Experimental results show the Densenet outperforms better than other state-of-art models under various measures.

Organization of paper: As we already came across brain tumor and their related information in Section 1, Section 2 describes the literature review, Section 3 describes the methodology, Section 4 depicts performance analysis and finally section 5 contains the conclusion part.

2. Literature Review

The Sharif et al. approach for categorizing multiclass brain tumors was proposed in 2022 [12]. To follow the advised line of action, the Densenet201 Pre-Trained DL Model is modified and trained using a deep transfer of unbalanced data learning. Two methods for the selection of features are provided because the traits of this layer are insufficient for precise categorization.

Kang et al. (2021) [13] retrieved deep features from brain MR images by using a large number of previously trained deep CNN. The extracted features are examined by different ML classifiers. They assess the efficacy of deep feature extractors, ML classifiers, and an ensemble of deep features for the classifying brain tumors using three separate brains MRI datasets that are freely available online.

A tripartite deep learning architecture was presented by Gunasekara et al. in 2021 [14]. On the recognized images, a region-based CNN (R-CNN) is subsequently applied to identify the cancer regions of interest. First, deep CNN are used to implement classifiers, and then R-CNN is used to localize tumor regions of interest on the classified images In order to create classifiers, deep convolutional neural networks are initially used. The concentrated tumor boundaries are contoured for the segmentation procedure in the third and final step using the Chan-Vese segmentation approach. A level set function-based active contour methodology is suggested since conventional edge detection techniques based on gradients of pixel intensity frequently fail during the segmentation process of medical images. The boundaries of the tumor were specifically established during segmentation using the Chan-Vese approach.

Deep learning algorithms are suggested by Gurunathan and Krishnan (2020) [15] as a strategy for automatically recognizing and identifying brain cancers in brain MRI images. Data augmentation is utilized as a preprocessing technique in this article. In this work, a segmentation method based on morphology was used to separate the cancer regions from the other categories of brain images. Additionally, the CNN is used to categorize the segmented tumor regions into "Mild" and "Severe" situations.

Polat and Gungen (2021) [16] proposed transfer learning networks as a method for classifying brain tumors via MR images. The "VGG16, VGG19, ResNet50, and DenseNet21" networks can be used to determine the kind of brain tumors that are most prevalent. Figshare dataset is used in this work and it contains 3065 T1-weighted MR images from almost 250 patients with different types of brain tumor such as glioma (almost 1500 images), meningioma (almost 800 images) and pituitary (almost 1000 images). For evaluating performance AUC and accuracy metrics are used. These four optimization methods such as "ADADETA, ADAM, RMSPROP, and SGD" (930 images) are used in this work.

Table 1. Overall summary of state-of-the-art models

Authors	Methodology	Limitations	Accuracy
Sharif et al. (2022)	Densenet 201	The elimination of several crucial characteristics that affect the system's accuracy.	97
Kang et al. (2021)	Ensemble network	Utilizing knowledge distillation techniques shrink the model for deployment on a real-time medical diagnosis system.	95
Gunasekara et al. (2021)	RCNN	Accuracy is low	93
Gurunathan & Krishnan (2020)	CNN	Tumor regions are identified in thermally scanned brain images. The complexity of the model is less while training.	95
Polat & Gungen (2021)	VGG16, VGG19, ResNet50 and DenseNet21	Small dataset problem leading towards over fitting.	95

2.1 Challenges and Research Gap

This research work is mainly focused on bringing an effective multi disease classification model by overcoming the following challenges;

- Existing models are trained in the way of a standalone system rather than giving further additional boosting stages for improving the efficiency
- Existing models are only classifying one type of tumors rather than multi-disease based which shows the level of detection of classifier
- As the standalone systems, the overall accuracy is comparatively less with others, in terms of using less complex classifiers as well
- Less use of other prior stages such as feature extraction, feature selection which is a potential efficiency incrementer.

3.Methodology

Figure 2 depicts the architecture of the proposed framework in which the following are the stages. For any deep learning model, sufficient data needs to be input to make the model understand the aspect. Thereby data collection is from multiple repositories to make a custom dataset which contains multiple brain tumor types. First data is collected, they are passed to b) Preprocessing stage where from the raw MRI images, anomalies and noises are removed using techniques like CLAHE (for brightness enhancing), Thresholding (Grayscale), Filtering (ADF) and skull masking. Once images are preprocessed, they undergo feature extraction for extracting quintessential features using PCA and then proceed to d) feature selection of those inputs using VGG16 and the output image classification is actioned using the Densenet164 network.

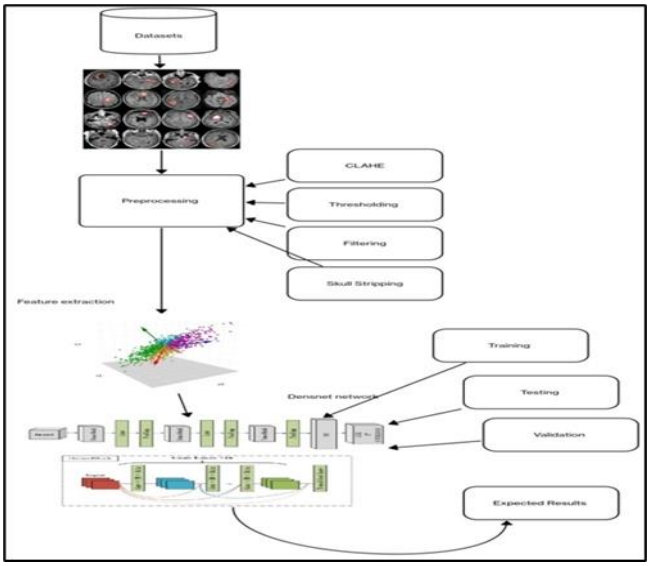

Fig 2. The architecture of the proposed system

3.1 Datatset Collection

For this research work, the data was collectively collected from the Kaggle repository where the type of brain tumors ("https://www.kaggle.com/datasets/jarvisgroot/brain-tumor-classification-mri-images"), Liver cancer (https://www.kaggle.com/datasets/robintrmbtt/data-unet) and Lung cancer (https://www.kaggle.com/datasets/hamdallak/the-iqothnccd-lung-cancer-dataset)

3.2Preprocessing

The preprocessing stage raises the caliber of the MR images of brain tumors and prepares them for upcoming processing by clinical professionals or imaging modalities. Additionally, it aids in enhancing MR image characteristics. In light of it, this work employs CLAHE, Grayscale, ADF, and skull masking approaches.

CLAHE: It was seen that the vast majority of the images in the datasets utilized in this study have low contrast. The images are upgraded with a common method called Contrast Limited Adaptive Histogram Equalization (CLAHE). A histogram of the gray values in a contextual zone centered on each pixel is first examined by CLAHE before assigning a value to each pixel's intensity within the display range [17]. It divides the histogram using a predetermined value known "clip limit" before calculating the Cumulative Distribution Function (CDF). The histogram's components that surpass the clip limit, however, are distributed uniformly throughout all histogram bins using CLAHE (Figure 3).

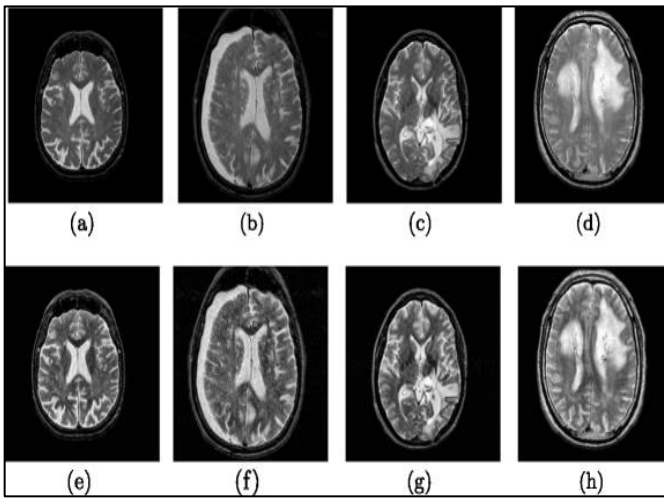

Fig 3. Preprocessed image after CLAHE Technique

Thresholding: The intensity values that represent the pixel values in a grayscale image range from 0 to 256. Figure 4 shows a grayscale image with several shades of gray ranging from black to white. Each pixel in a grayscale image has a specific electromagnetic spectrum region where the light intensity is concentrated. A color image is converted to grayscale using varying weights for the red, green, and blue color channels to accurately replicate the effect of shooting black-and-white film. The fact that the RGB image and the grayscale image share the same luminance is one way they can be compared.

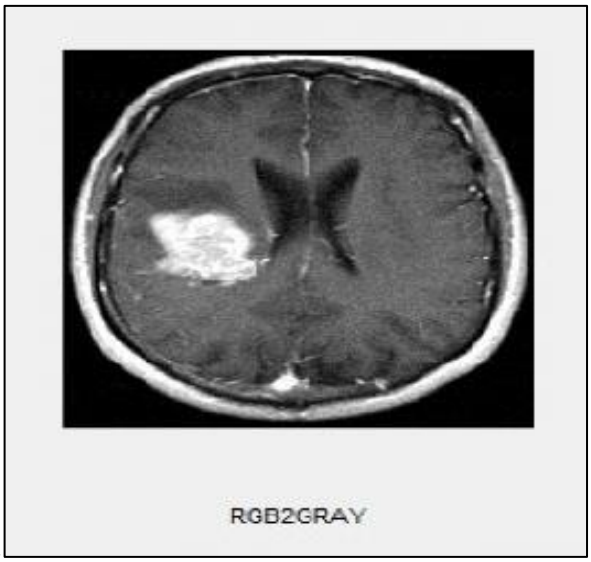

Fig 4. Preprocessing using Grayscale conversion

Filtering: Anisotropic Diffusion Filter (ADF), skull stripping, and contrast boosting are procedures in image preprocessing. After skull stripping to remove extraneous tissues from MR images and contrast enhancement to boost visual clarity, ADF removes noise content from the pictures while maintaining the borders of existent objects.

The main goal of the noise-reduction technique used for preprocessing images is to improve the features of damaged images by removing noise [19]. Denoising is done using the regional noise information that is present in the image in the case of adaptive filtering. Before continuing, it is important to remember that the reduced image is defined by I(x,y), that y2 represents the variance of the noise image as a whole, that L provides the mean of local around a window pixel, that y2 provides the variance local in a window, and that y2 provides the mean of local in a window.

$$\hat{I}(x,y) - \frac{\sigma_y^2}{\hat{\sigma}_y^2}\left(\hat{I}(x,y) - \hat{\mu}L\right) \quad (1)$$

If the noise variance in the image is near to zero,

$$\sigma_y^2 = 0 => \hat{I} = \hat{I}(x,y) \quad (2)$$

If the local variation is bigger than the global difference and the global noise variance is minor, the ratio is either one or one.

$$\hat{\sigma}_y^{2"}\sigma_y^2, then\ I = I(x,y) \quad (3$$

A large local variance characterizes the emergence of an edge in the investigated image window. When the local and global variations are almost similar it can be expressed as

$$\hat{I} = \hat{\mu}Las\hat{\sigma}_y^2 \approx \sigma_y^2 \quad (4)$$

The result is simply displayed above analogies and reflects the mean value of the window over the length of a pixel. It is a typical application in a healthy area. If no irregularities are found, the outcome gains an advantage. This

characteristic is necessary for an adaptive filter. Based on the input image and window size, the filter controls the balance. Figure 5 represents the results of the experiment on noise removal in images of brain tumors using an adaptive filter.

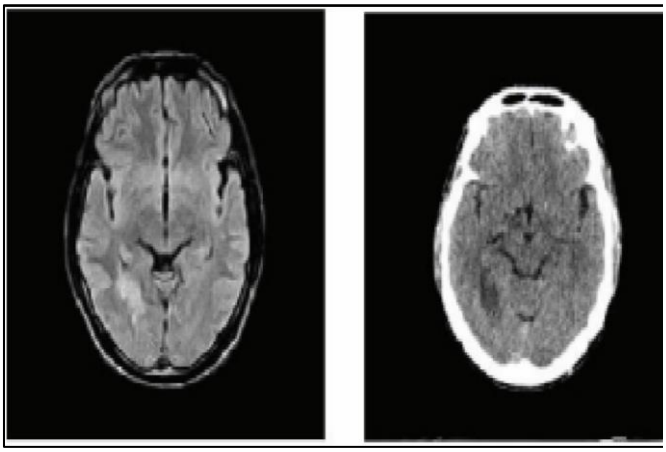

Fig 5. Preprocessing after the ADF filtering technique

Skull stripping: In order to generate the image required for tumor diagnosis, skull stripping is the process of eliminating unwanted and non-brain-related portions of scanned images. The scanned image shows the dura, scalp, skull, and brain region. A Cerebrospinal Fluid (CSF) rim can assist in isolating the unwanted components. The skull can be removed and the required brain area can be obtained using intensity thresholding and morphological surgery. This will allow for the identification of the tumor. Let's say that the input image can be expressed by an array of pixels that contain the intensity values at specific locations within the image.

Let Ip={ Ip1, Ip2..Ipn} where Ip1... Ipn stands for the intensities of pixels 1 through n. Additionally, np denotes the overall number of pixels in an image. Set the intensity threshold to T, and the requirement for removing pixels from the image is that they must have intensity below T. Typically, the narrow connections would be represented by those pixels meeting this criterion. The technique is set up to meet two requirements. One is that non-brain structures should have weak connections to the brain [20]. The second is that as much brain as feasible should be preserved by the intensity thresholding mask. In this situation, choosing the threshold value is crucial because if it is set too low, dura may be included, which is undesirable. A clearer distinction between the brain and non-brain structures may be possible with excessive threshold levels, but at the cost of brain deterioration. Therefore, to get good results, the threshold should be set at the optimum level. We now have the necessary brain image after intensity thresholding, but it still needs to be improved in order to be suitable for tumor detection methods. We employ morphological operations for this. Additionally, it helps to get rid of tight connections.

3.3 Feature extraction

To reduce the dimensionality of huge datasets, PCA is a feature extraction technique that identifies the eigenvectors of a covariance matrix with the highest eigen values. In order to determine the tumor area obtaining the greatest amount of data variance, it extracts the similarities and differences from a sizable dataset. The following is the PCA definition in algebra: [21]

a. To get the mean for the data framework, do the following:

$$\mu = E(D) \qquad (5$$

And then, calculate the covariance as follows:

$$CV = Cov(D) = E[(D - \mu)(D - \mu)^T] \qquad (6)$$

b. Count the eigenvalue and eigenvector e1, e2,e3.., eN, 1,2,.....N of the covariance CV, sorting the eigenvalue in descending order, solve the equation for the covariance CV as follows:

$$|\lambda I - CV| = 0 \qquad (7)$$

Where I refer to the identity matrix as the CV's similar dimension. Using Singular Value Decomposition (SVD), obtain the eigenvalues, 1>=2 >=>=.. k and e-k (k=1,2, M) eigenvectors [22]. In order to select the k for obtaining principal components, we count the percentage of the data covered by the first M eigenvalues. The weight matrix Wm is calculated by the below formula, whose columns are DtD eigenvectors:

$$W_m = \frac{\sum_{i=1}^{M} \lambda_k}{\sum_{=1^{\wedge}}^{M} \alpha\, \lambda_k} \qquad (8)$$

decide on the main M eigenvalue that increased the total extent to 85% as the principal segment.

c.Information extended to a lower measurement subspace ,

$$P = W^T X \qquad (9)$$

where X stands for the scaled version of the original data and T stands for the transpose matrix. We can reduce the number of elements or measures from n to M by making use of the main eigenvector that affects each unique M [23].

The evaluation of the distinct stages of the tumor (tumor staging) and the diagnosis could all benefit from textural observations and analysis. Table 2 provides a list of some of the essential features along with their statistical feature formulas.

Table 3. Overall statistical features for feature extraction

Statistical features	**Calculation**
Mean (M). By dividing the total number of pixels by the sum of all the pixel values in the image, the mean of the image is determined.	$M = \left(\frac{1}{m*n}\right)\sum_{x=0}^{m-1}\sum_{y=0}^{-1}(X, Y)$ (10)
Standard Deviation (SD). The second central moment characterising the probability distribution of an observed population is the standard deviation, a measure of inhomogeneity. An image's edges have great contrast and a superior intensity level when the value is higher.	SD(σ) $= \left(\frac{1}{m*n}\right)\sum_{x=0}^{m-1}\sum_{y=0}^{n-1}(f\ (x,y) - M)^2$ (11)
Entropy (E). Entropy is a determined indicator of a textural image's randomness and is described as:	$E = -\sum_{x=0}^{m-1}\sum_{y=0}^{n-1} f\ (x,y).log_2 f(x,y).$ (12)
Skewness (Sk(X)). Skewness is a metric for symmetry or lack of how skewed a random variable is. The symbol for Sk is Sk (X), and its definition is:	$S_k(X) = \left(\frac{1}{m*n}\right)\frac{\sum(f(x,y)-M)^3\|}{SD^3}$ (13)
Kurtosis (Sk). You can use the Kurtosis parameter to describe how a random variable's probability distribution works. Kurt is the name of the Kurtosis for the random variable X. (X), and it is defined as	$K_{urt}(X) = \left(\frac{1}{m*n}\right)\frac{\sum(f(x,y)-M)^4\|}{SD^4}$ (14)
Energy (En). Energy is the quantifiable sum of the number of repeated pixel pairs. A statistic called energy is used to compare two photographs. The "angular second moment," which is commonly referred to as "energy" if the Haralicks GLCM feature is utilized to characterise it, is defined as:	$En = \sqrt{\sum_{x=0}^{m-1}\sum_{y=0}^{n-1} f^2(x,y).}$ (15)
Contrast (Con). The definition of contrast, which is a measurement of the intensity of a pixel and its neighbour throughout the image is:	$C_{on} = \sum_{x=0}^{m-1}\sum_{y=0}^{n-1}(x-y)^2 f(x,y).$ (16)
Inverse Difference Moment or Homogeneity (IDM). The Inverse Difference Moment assesses an image's local homogeneity. IDM may have a single value or a range of values to indicate whether or not an image is textured.	$IDM = \sum_{x=0}^{m-1}\sum_{y=0}^{n-1}\frac{1}{1+(x-y)^2} f(x,y).$ (17)
Directional moment (DM). Using the alignment of the image as a gauge for angle, the definition of the directional moment, a textural attribute of an image is as follows:	$DM = \sum_{x=0}^{m-1}\sum_{y=0}^{n-1} f(x,y)\|x-y\|.$ (18)
Correlation (Corr). In order to describe the spatial interdependence between the pixels, a correlation feature is defined as:	$C_{orr} = \frac{\sum_{x=0}^{m-1}\sum_{y=0}^{n-1}(x,y)f(x,y)-M_x M_y}{\sigma_x \sigma_y}$ (19)

3.4 Classification using Densenet

MRI images are frequently used to find brain tumors. Patient I is represented by the 2-D image sequence Xi = x(i) 1, ••, x(i) T, with x(i) t R-1-2 serving as the t-th frame image. In contrast to earlier label-exhaustive datasets, each 2-D image was linked with a label, in our dataset, each sequence of images Xi is associated with a single label yi 0, 1, •••, P, where P denotes cancer types number. Thus, the representation of our dataset is D - (Xi, yi)N i=1, where N denotes the image sequence number in total.

The VGG16 network is used as a feature to choose necessary features from the extraction process in order to enable the classifier network better predict the input. The most recent special convolutional neural network variation,

called DenseNet [24–28], connects the current layer to every layer before it. In a deep DenseNet, additional convolutional and pooling procedures are carried out between neighbouring dense blocks in addition to the sequential connections between the dense blocks in a DenseNet. With such a topology, we can build a deep neural network that is flexible enough to explain complex transitions. Figure 6 shows a deep DenseNet in illustration form.

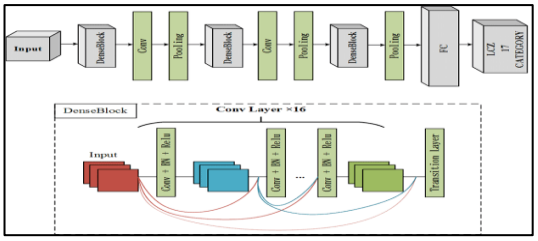

Fig 6. Densenet201 architecture for the proposed system

4. Performance Analysis

Software prerequisites include Google Collaboratory, an open-source Google environment, and Pytorch, the open-source Python library for creating deep learning models. The model is implemented using hardware requirements such as a Ryzen 5/6 series CPU, NV GTX, 1 TB HDD, and Windows 10 OS. Experimental evaluation of measures such as accuracy, sensitivity, specificity, recall, precision, F1-score, detection rate, TPR, FPR, and confusion matrix was done using cutting-edge models. Table 4 displays a comparison of models. Figure 7 illustrates how the suggested system performs better than previous models in terms of accuracy, sensitivity, and specificity (a,b,c) because of its sophisticated structural design and the manner it was trained using appropriate training parameters.

Table 4. Comparative analysis of accuracy, sensitivity, specificity

Models	Accuracy	Sensitivity	Specificity	Images
Sharif et al. (2022)	97	96	97	
Kang et al. (2021)	95	97	98	
Gunasekara et al. (2021)	93	96	97	Image 1
Gurunathan & Krishnan (2020)	95	97	98	
Polat & Gungen (2021)	95	98	98	
Proposed system	98	99	99	

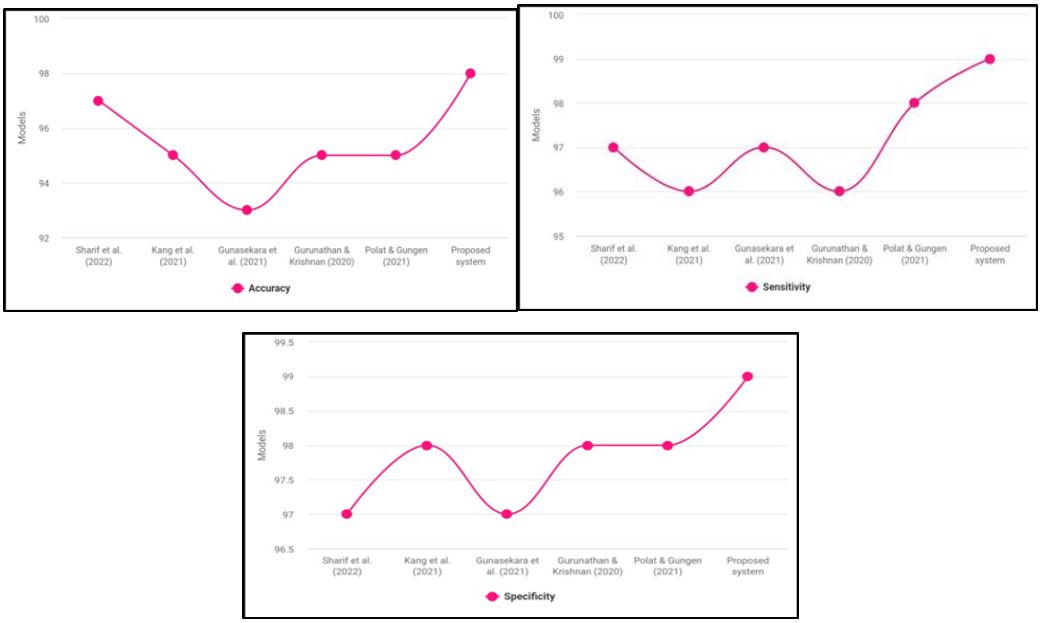

Fig 7. Models vs a) accuracy, b) Sensitivity c) Specificity

Table 5 depicts a comparison analysis of models. Figure 8(a,b,c)shows a graphical representation of several models over precision, recall, and f1-score in which the proposed system outperforms better due to the custom dataset which

contains a large amount to train the model to understand the various types of brain tumor for classifying. Also the quality of the image where the classifier can predict and perform better than other models.

Table 5. Comparative analysis of Precision, Recall, F1-score

Models	Precision	Recall	F1-score	Images
Sharif et.al.(2022)	82	86	90	
Kangetal.(2021)	85	90	94	
Gunasekaraetal.(2021)	87	92	96	Image1
Gurunathan&Krishnan(2020)	88	93	97	
Polat&Gungen(2021)	85	90	94	
Proposed system	89	94	98	

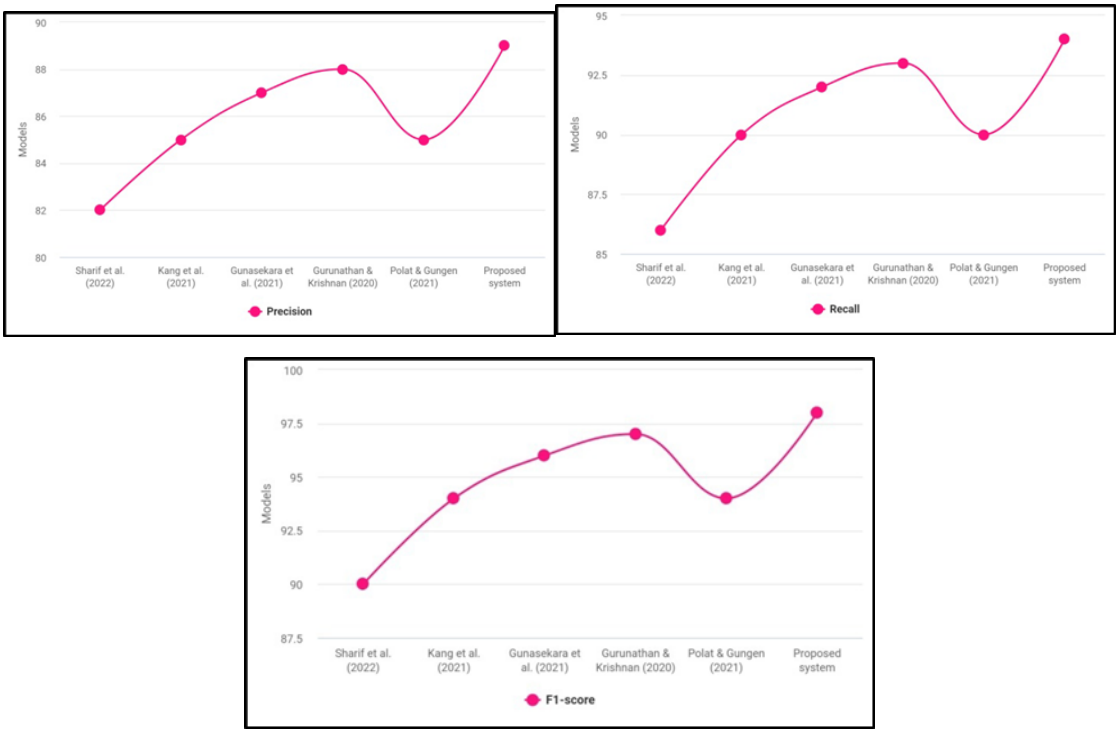

Fig 8. Models vs a) Precision, b) Recall, c) F1-score

Table 6 depicts a comparison analysis of models. Figure 9(a,b,c) shows a graphical representation of several models over detection rate, TPR, and FPR in which the proposed system outperforms better due to VGG16 acting as a feature selector where it's a pre-trained model on ImageNet which acts as transfer learning improving or boosting the knowledge of Densnet network on those inputs.

Table 6. Comparative analysis of Detection rate, True Positive Rate, False Positive Rate

Models	Detection rate	TPR	FPR	Images
Sharifetal.(2022)	91.4	87	13	
Kangetal.(2021)	87.8	83	17	
Gunasekaraetal.(2021)	89.8	84	16	Image1
Gurunathan&Krishnan(2020)	92.5	87	13	
Polat&Gungen(2021)	93.7	88	12	
Proposed system	94	90	10	

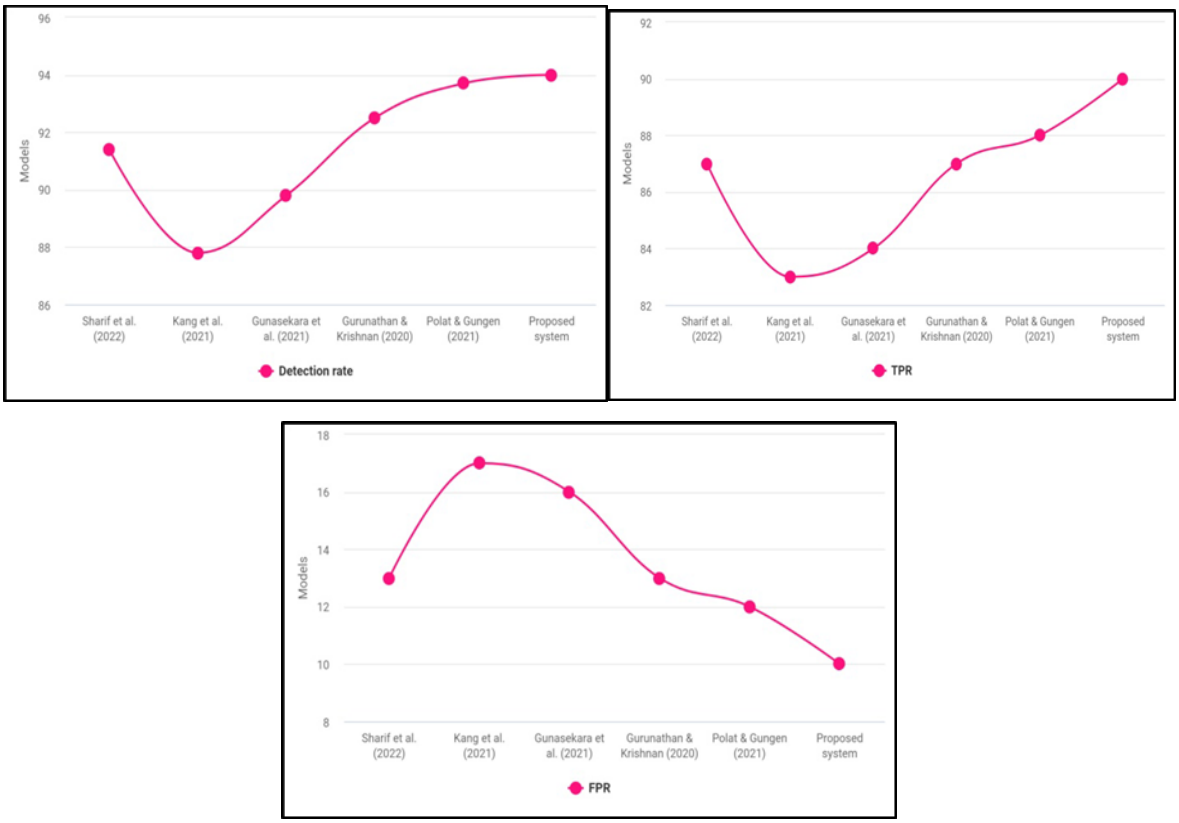

Fig 9. Models vs a) Detection rate, b) TPR, c) FPR

Figure 10 shows the output obtained from the Densnet network. Figure 11 represents the confusion matrix of the proposed system obtained. Figure 12 (a,b) shows the accuracy and loss of the proposed model during training. From figure 12a, it's clear that accuracy is getting exponentially increased as the validation continues to be static. While 12b shows as the validation is been statically low, the loss of the proposed system exponentially decreases which is a mirror image of the accuracy image. Figure 13 shows the epoch range parameters in the Google collaboratory environment.

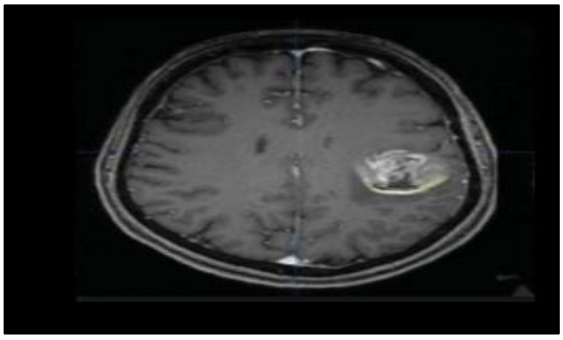

Fig 10. Output instances after being classified through the proposed system

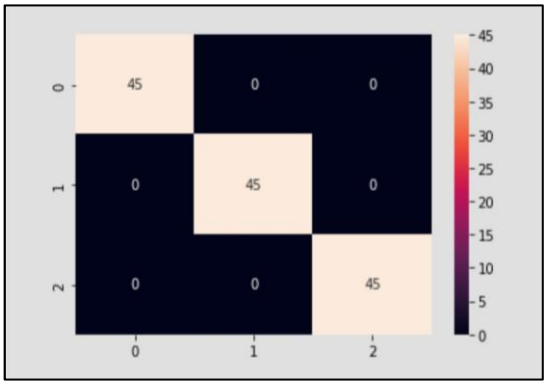

Fig 11. Confusion matrix of the proposed system

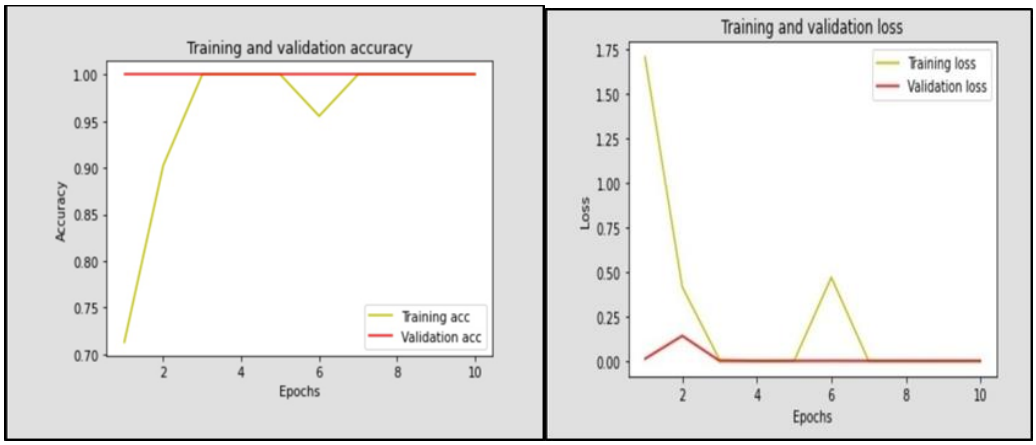

Fig 12. Proposed system on a) Accuracy, b) Loss during training and validation period

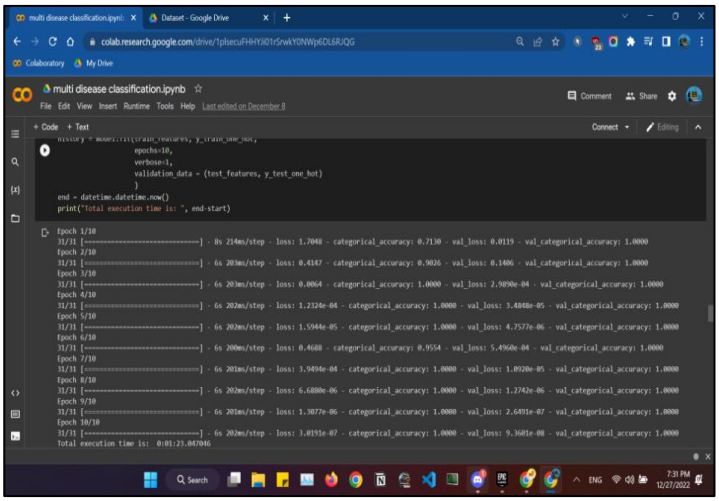

Fig 13. Epoch range on training the proposed framework

5. Conclusion

In this research work, the method to detect and classify multiple brain tumor types is done. Initially, data is collected from popular repositories and custom datasets to improve the efficiency of training and then it undergoes preprocessing techniques to improve the quality of the image to be predicted and is passed for PCA extracting features for classifier densenet to understand and learn to classify brain tumors. With the immense usage of such advanced techniques, we have eradicated the limitations that current state-of-the-art models faced. In future work, the usage of an additional network to integrate this system as a hybrid mode where transfer learning using pre-trained models can be used to improve the efficiency overhttp://www.bookref.com.

References

[1] M. Akil, R. Saouli, and R. Kachouri, "Fully automatic brain tumor segmentation with deep learning-based selective attention using overlapping patches and multi-class weighted cross-entropy," Medical Image Analysis, vol. 63, Article ID 101692, 2020.

[2] H. Habib, R. Amin, B. Ahmed, and A. Hannan, "Hybrid algorithms for brain tumor segmentation, classification and feature extraction," Journal of Ambient Intelligence and Humanized Computing, vol. 119, pp. 1–22, 2021.

[3] M. N. Ullah, Y. Park, G. B. Kim et al., "Simultaneous acquisition of ultrasound and gamma signals with a single-channel readout," Sensors, vol. 21, no. 4, p. 1048, 2021.

[4] F. Jamil, M. A. Iqbal, R. Amin, and D. Kim, "Adaptive thermal-aware routing protocol for wireless body area network," Electronics, vol. 8, no. 1, p. 47, 2019

[5] S. Deepak and P. Ameer, "Brain tumor classification using deep CNN features via transfer learning," Computers in Biology and Medicine, vol. 111, Article ID 103345, 2020.

[6] Mohsen, H., El-Dahshan, E. S. A., El-Horbaty, E. S. M., & Salem, A. B. M. (2018). Classification using deep learning neural networks for brain tumors. Future Computing and Informatics Journal, 3(1), 68-71.

[7] Almadhoun, H. R., & Abu-Naser, S. S. (2022). Detection of Brain Tumor Using Deep Learning.

International Journal of Academic Engineering Research (IJAER), 6(3).

[8] Siar, M., & Teshnehlab, M. (2019, October). Brain tumor detection using deep neural network and machine learning algorithm. In 2019 9th international conference on computer and knowledge engineering (ICCKE) (pp. 363-368). IEEE.

[9] Naser, M. A., & Deen, M. J. (2020). Brain tumor segmentation and grading of lowergrade glioma using deep learning in MRI images. Computers in biology and medicine, 121, 103758.

[10] Sun, L., Zhang, S., Chen, H., & Luo, L. (2019). Brain tumor segmentation and survival prediction using multimodal MRI scan with deep learning. Frontiers in neuroscience, 13, 810.

[11] Alqudah, A. M., Alquraan, H., Qasmieh, I. A., Alqudah, A., & Al-Sharu, W. (2020). Brain tumor classification using deep learning technique--a comparison between cropped, uncropped, and segmented lesion images with different sizes. arXiv preprint arXiv:2001.08844.

[12] Sharif, M. I., Khan, M. A., Alhussein, M., Aurangzeb, K., & Raza, M. (2022). A decision support system for multimodal brain tumor classification using deep learning. Complex & Intelligent Systems, 8(4), 3007-3020.

[13] Kang, J., Ullah, Z., & Gwak, J. (2021). Mri-based brain tumor classification using an ensemble of deep features and machine learning classifiers. Sensors, 21(6), 2222.

[14] Gunasekara, S. R., Kaldera, H. N. T. K., & Dissanayake, M. B. (2021). A systematic approach for MRI brain tumor localization and segmentation using deep learning and active contouring. Journal of Healthcare Engineering, 2021.

[15] Gurunathan, A., & Krishnan, B. (2021). Detection and diagnosis of brain tumors using deep learning convolutional neural networks. International Journal of Imaging Systems and Technology, 31(3), 1174-1184. [16] Polat, Ö., & Güngen, C. (2021). Classification of brain tumors from MR images using deep transfer learning. The Journal of Supercomputing, 77(7), 7236-7252.

[16] Thillaikkarasi, R., & Saravanan, S. (2019). An enhancement of deep learning algorithm for brain tumor segmentation using kernel-based CNN with M-SVM. Journal of medical systems, 43(4), 1-7.

[17] Abd Khalid, N. E., Ismail, M. F., Manaf, M. A. A., Fadzil, A. F. A., & Ibrahim, S. (2020). MRI brain tumor segmentation: A forthright image processing approach. Bulletin of Electrical Engineering and Informatics, 9(3), 1024-1031.

[18] Maurya, R., & Wadhwani, S. (2022). An efficient method for brain image preprocessing with anisotropic diffusion filter & tumor segmentation. Optik, 265, 169474.

[19] Rajesh, M. (2021). Preprocessing and Skull Stripping of Brain Tumor Extraction from Magnetic Resonance Imaging Images Using Image Processing. Recent Trends in Intensive Computing, 39, 299.

[20] Gaikwad, S. B., & Joshi, M. S. (2015). Brain tumor classification using principal component analysis and probabilistic neural network. International Journal of Computer Applications, 120(3).

[21] Hamid, M. A., & Khan, N. A. (2020). Investigation and classification of MRI brain tumors using feature extraction technique. Journal of Medical and Biological Engineering, 40(2), 307-317.

[22] Gumaei, A., Hassan, M. M., Hassan, M. R., Alelaiwi, A., & Fortino, G. (2019). A hybrid feature extraction method with regularized extreme learning machine for brain tumor classification. IEEE Access, 7, 36266-36273.

[23] Zhou, Y., Li, Z., Zhu, H., Chen, C., Gao, M., Xu, K., & Xu, J. (2018, September). Holistic brain tumor screening and classification based on densenet and recurrent neural network. In International MICCAI Brainlesion Workshop (pp. 208-217). Springer, Cham.

[24] Nawaz, M., Nazir, T., Masood, M., Mehmood, A., Mahum, R., Khan, M. A., & Thinnukool, O. (2021). Analysis of brain MRI images using improved cornernet approach. Diagnostics, 11(10), 1856.

[25] Hu, J., Gu, X., & Gu, X. (2021). Dual-pathway DenseNets with fully lateral connections for multimodal brain tumor segmentation. International Journal of Imaging Systems and Technology, 31(1), 364-378.

[26] Masood, M., Nazir, T., Nawaz, M., Mehmood, A., Rashid, J., Kwon, H. Y., & Hussain, A. (2021). A novel deep learning method for recognition and classification of brain tumors from MRI images. Diagnostics, 11(5), 744.

[27] Kalpana, R., Bennet, M. A., & Rahmani, A. W. (2022). Metaheuristic OptimizationDriven Novel Deep Learning Approach for Brain Tumor Segmentation. BioMed Research International, 2022.

[28] Sudeepthi Govathoti, A Mallikarjuna Reddy, Deepthi Kamidi, G BalaKrishna, Sri Silpa Padmanabhuni and Pradeepini Gera, “Data Augmentation Techniques on Chilly Plants to Classify Healthy and Bacterial Blight

Disease Leaves" International Journal of Advanced Computer Science and Applications(IJACSA), 13(6), 2022. http://dx.doi.org/10.14569/IJACSA.2022.0130618

[29] V. NavyaSree, Y. Surarchitha, A. M. Reddy, B. Devi Sree, A. Anuhya and H. Jabeen, "Predicting the Risk Factor of Kidney Disease using Meta Classifiers," *2022 IEEE 2nd Mysore Sub Section International Conference (MysuruCon)*, 2022, pp. 1-6, doi: 10.1109/MysuruCon55714.2022.9972392.

[30] B. H. Rao *et al*., "MTESSERACT: An Application for Form Recognition in Courier Services," *2022 3rd International Conference on Smart Electronics and Communication (ICOSEC)*, 2022, pp. 848-853, doi: 10.1109/ICOSEC54921.2022.9952031

[31] P. S. Silpa *et al*., "Designing of Augmented Breast Cancer Data using Enhanced Firefly Algorithm," *2022 3rd International Conference on Smart Electronics and Communication (ICOSEC)*, 2022, pp. 759-767, doi: 10.1109/ICOSEC54921.2022.9951883.

[32] P. Grandhe, A. M. Reddy, K. Chillapalli, K. Koppera, M. Thambabathula and L. P. Reddy Surasani, "Improving The Hiding Capacity of Image Steganography with Stego-Analysis," 2023 IEEE International Conference on Integrated Circuits and Communication Systems (ICICACS), Raichur, India, 2023, pp. 01-06, doi: 10.1109/ICICACS57338.2023.10100146.

[33] Jenifa Sabeena, S. ., & Antelin Vijila, S. . (2023). Moulded RSA and DES (MRDES) Algorithm for Data Security. International Journal on Recent and Innovation Trends in Computing and Communication, 11(2), 154–162. https://doi.org/10.17762/ijritcc.v11i2.6140

[34] Prof. Prachiti Deshpande. (2016). Performance Analysis of RPL Routing Protocol for WBANs. International Journal of New Practices in Management and Engineering, 5(01), 14 - 21. Retrieved from http://ijnpme.org/index.php/IJNPME/article/view/43

[35] Aoudni, Y., Donald, C., Farouk, A., Sahay, K. B., Babu, D. V., Tripathi, V., & Dhabliya, D. (2022). Cloud security based attack detection using transductive learning integrated with hidden markov model. Pattern Recognition Letters, 157, 16-26. doi:10.1016/j.patrec.2022.02.012